Bioconjugate Chemistry

Article

pubs.acs.org/bc

Fluorescent Functionalization across Quaternary Structure in a Virus-like Particle

Zhuo Chen,[†] Stefanie D. Boyd,[‡] Jenifer S. Calvo,[†] Kyle W. Murray,[†] Galo L. Mejia,[§] Candace E. Benjamin,[†] Raymond P. Welch,[†] Duane D. Winkler,[‡] Gabriele Meloni,[†] Sheena D'Arcy,[†] and Jeremiah J. Gassensmith*[,†]

[†]Department of Chemistry and Biochemistry, [‡]Department of Biological Sciences, and [§]School of Behavioral and Brain Sciences, University of Texas at Dallas, Richardson, Texas 75080, United States

Supporting Information

ABSTRACT: Proteinaceous nanomaterials and, in particular, virus-like particles (VLPs) have emerged as robust and uniform platforms that are seeing wider use in biomedical research. However, there are a limited number of bioconjugation reactions for functionalizing the capsids, and very few of those involve functionalization across the supramolecular quaternary structure of protein assemblies. In this work, we exploit the recently described dibromomaleimide moiety as part of a bioconjugation strategy on VLP Qβ to break and rebridge the exposed and structurally important disulfides in good yields. Not only was the stability of the quaternary structure retained after the reaction, but the newly functionalized particles also became brightly fluorescent and could be tracked in vitro using a commercially available filter set. Consequently, we show that this highly efficient bioconjugation reaction not only introduces a new functional handle "between" the disulfides of VLPs without compromising their thermal stability but also can be used to create a fluorescent probe.

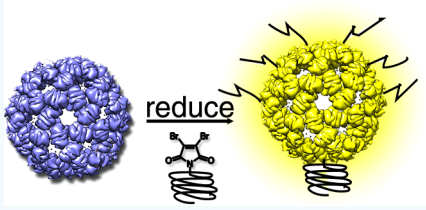

INTRODUCTION

Over the preceding two decades, nanoparticles have taken a prominent position in biomedical research,[1−5] and among the various compositions of nanoparticles, virus-like particles (VLPs), the noninfectious proteinaceous derivatives of viruses, stand out as being both highly functionalizable and biodegradable[6−11] because they will be eliminated by the reticuloendothelial system and cleared from the body.[12] VLPs are self-assembled macromolecular structures comprising anywhere from several dozen to thousands of individual protein subunits.[13] This higher-order quaternary structure has been exploited both chemically[14−18] and genetically[19,20] to create new materials such as drug carriers,[7,21−23] bright fluorescent probes,[24−28] long T1 MRI contrast agents,[29−33] PET radiotracers,[34] and platforms for vaccine development.[35−37] Bacteriophage Qβ, which is a 28 nm icosahedral protein nanoparticle, is one such VLP that has been widely investigated as a template for nanomedicine.[29,30,38] The capsid self-assembles around RNA from 180 identical coat proteins, in which two monomers are tightly interlocked through hydrophobic interactions. These 90 dimers are linked together by disulfides between Cys74 and Cys80 and self-assembled into icosahedral particles. The individual 14.2 kDa coat proteins are composed of 132 amino acids, of which four solvent exposed primary amines on the exterior surface have been used as reaction sites to install fluorescent labels,[15] contrast agents,[31,32] therapeutic drugs,[18] and polymer initiators.[15,39] While additional functionalities can be programmed via site-selective mutagenesis, there is an articulated[40] need to develop additional and orthogonal reaction methods that functionalize VLPs for new technologies in targeted drug delivery and imaging applications.

One exploitable functional group is disulfide bridges, which are surprisingly common in viral capsids.[41] For instance, coliphage (groups III and IV), *Pseudomonas* phage P77, hepatitis B and C, and HIV possess disulfide functional groups located on their surfaces.[42] An issue with utilizing disulfides as functional handles, however, is that reduction of the disulfide bond to free cysteines usually decreases the thermal stability of the tertiary structure of the folded protein monomer.[43] In some of the aforementioned VLPs, the disulfides are involved in stabilizing the larger supramolecular (quaternary) structure as well by offering a covalent link between the individual monomers, strengthening the overall superstructure of the virus.[43,44] Indeed, such is the case in Qβ, which possesses 180 solvent exposed disulfide groups lining each pore connecting either five or six protein monomers in a daisy-chain fashion (Figure 1). Recently, dibromomaleimide (DB) derivatives have emerged as a means of functionalizing disulfides by reacting specifically with two free thiols obtained from the reduction of a single disulfide to form a two-carbon bridge. This reaction has been used to rebridge reduced disulfides on small peptides[45] and proteins,[46,47] and we recently communicated a strategy employing DB conjugates to attach polymers to improve the solubility of photolytically activated doxorubicin−Qβ conjugate.[18] In this article, we expand upon this reaction and show

Received: June 1, 2017
Revised: July 30, 2017
Published: August 8, 2017

DOI: 10.1021/acs.bioconjchem.7b00305
Bioconjugate Chem. 2017, 28, 2277−2283

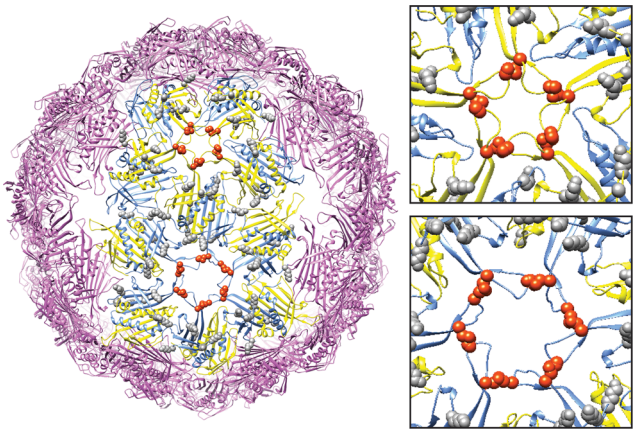

Figure 1. Crystallographic structure of Qβ VLP (PDB ID: 1QBE). Cysteine residues (Cys 74 and Cys 80 shown in red) are located along the pores. These cysteines form disulfide bridges that link 5 monomers (top insert) or 6 monomers (bottom insert) to create a total of 32 pore structures on the capsid.

that cationic, anionic, polymeric, and neutral small-molecule DB derivatives attach to the capsids in good yields while retaining the thermal stability afforded by the original disulfide bond. In addition, we also show that alkyl-substituted DB functional groups become fluorescent following displacement of the bromides by the capsid thiol groups and this reaction produces a fluorescent probe with incredibly fast kinetics. This single moiety permits the introduction of bespoke functionality and provides a turn-on response following reaction with disulfides yielding a fluorescent probe suitable for imaging in vitro.

RESULTS AND DISCUSSION

The preparation of DB derivatives is synthetically straightforward and achieved via the condensation of dibromomaleic anhydride with a primary amine possessing the desired functional group. To test the scope of the DB conjugation to Qβ, a series of DB derivatives (Scheme 1) was prepared as detailed in the Supporting Information.

The pentameric and hexameric subunits of the VLP Qβ (Figure 1) are linked by disulfides, all of which are solvent exposed. Upon the addition of 5 equivalents of tris(2-carboxyethyl)phosphine (TCEP) at room temperature (RT) for 1 h, all 180 disulfides are reduced to the corresponding 360 free thiol functional groups. This reduction, confirmed using nonreducing sodium dodecyl sulfate polyacrylamide gel electrophoresis (SDS-PAGE, Figure 2A) shows that, following the addition of five equivalents of TCEP, the higher-order oligomers are mostly gone, an observation consistent with literature reports.[18] A pair of notable features of the gel bear explanation: (1) a strongly associated dimer persists following reduction and denaturation. This dimer is noncovalently associated and difficult to eliminate, an observation that has been reported elsewhere.[44,49] (Tight noncovalent interactions between monomers of Leviviridae RNA phages, of which Qβ is a member, are observed commonly; see ref 48.) (2) Visible in the control lane containing zero TCEP are some lower-order oligomers of the pore structures, and protein monomer can be seen. Size-exclusion chromatography by fast protein liquid chromatography (FPLC; Figure 2B) shows a single peak corresponding to pure capsid, indicating that these lower-order oligomers are not impurities left over following expression but

Scheme 1. Qβ Reduction and DB Compounds[a]

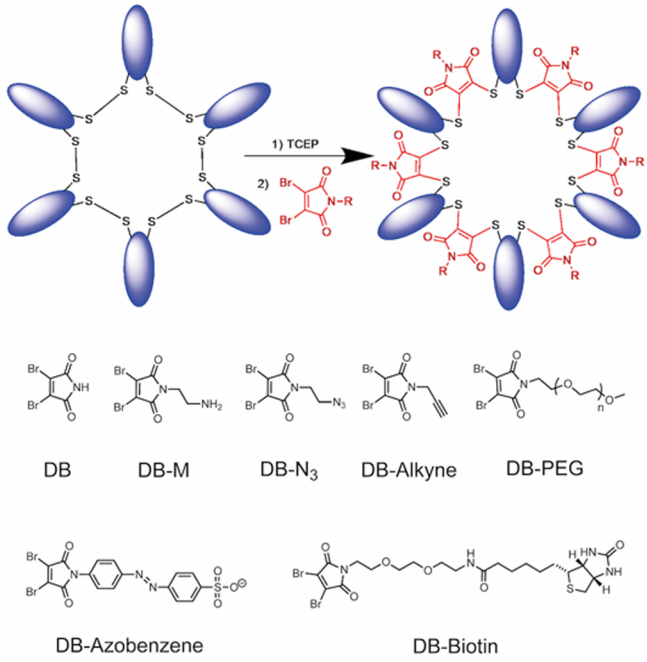

[a]The DB compound reacts with the thiol function in the reduced Qβ to form the corresponding Qβ–maleimide conjugates.

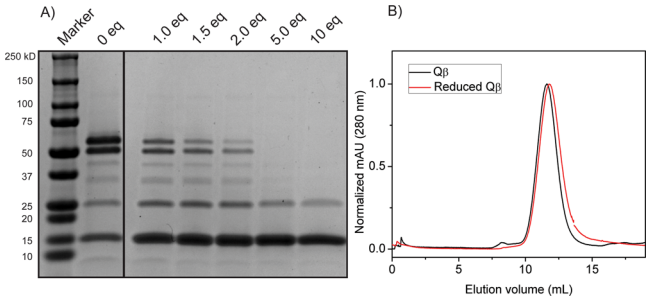

Figure 2. (A) Nonreducing SDS-PAGE showing the extent of reduction with different equivalents of TCEP. This analysis shows that, after Qβ is incubated with 5 equivalents of TCEP at RT for 1 h, all of the higher-order structures are reduced. Dimers present in the gel are formed by hydrophobic interactions, not disulfide bonds. (B) FPLC traces of Qβ (11.6 mL) and reduced Qβ (11.7 mL).

rather suggest incomplete post-translational disulfide oxidation. We were able to partially confirm this with Ellman's assay, a colorimetric assay used to quantify free thiol groups on proteins, which showed that about 10% of the disulfides on the as-expressed VLP are actually already reduced and present as free thiol groups. We were able to further confirm this when the as-expressed capsid was treated with a 7 mM solution of hydrogen peroxide, which elevated the oxidized disulfides from 88.2% to 98.2% (Figure S11). Complete reduction, such that all 180 disulfides are free thiols, does not change the apparent size of the capsid, as shown by FPLC in Figure 2B, and it remains stable in buffer for many hours. (Figure S13)

Because the phosphine-based reducing agent TCEP is insufficiently reactive against the dibromomaleimide groups, the reduction and addition of the DB conjugates can occur in a single pot. After a 1 h incubation period with TCEP, 20 equiv of the desired DB compound are added directly to the Qβ solution. The reaction is then allowed to proceed overnight,

DOI: 10.1021/acs.bioconjchem.7b00305
Bioconjugate Chem. 2017, 28, 2277–2283

followed by purification using centrifugal filter (MWCO = 10 kDa, centrifuged at 4300 rpm at 4 °C with the exchange of buffer three times to remove small molecules). TCEP is used as a reducing agent because traditional thiol-based reducing agents reverse the reaction via a thiol addition−elimination mechanism. This observation begged the question if cysteine-rich substrates in plasma might undo any conjugates in vitro. A report by Nunes et al.[50] found that, while the maleimide conjugates could be removed in serum, hydrolysis of the maleimides to their corresponding maleamic acids prevented this. We tested the stability of the conjugates in serum using Qβ−alkyne with a fluorescein isothiocyanate dye attached via click reaction and were pleased to see that, after incubation of the conjugates at pH 8.2 for 24 h, we were able to approximate the literature results on our VLP with significantly less transfer of the hydrolyzed functional group in serum after incubating for 24 h at 37 °C (the procedure is detailed in the Serum Stability Studies section in the Supporting Information).

Apart from Qβ−azobenzene, reaction yields were inferred by measuring the remaining free thiols using Ellman's assay immediately following workup. Because the Qβ−azobenzene absorbs at 500 nm, which overlaps with the colored Ellman's assay product 2-nitro-5-thiobenzoic acid (TNB), the yield of this reaction had to be determined by densitometry. The yields are typically good, with approximately 117−152 of the 180 disulfides being functionalized following our reaction procedure (Table 1). (The presence of TCEP during the Qβ and DB−

Table 1. DB Compound Rebridging of Disulfides on Qβ

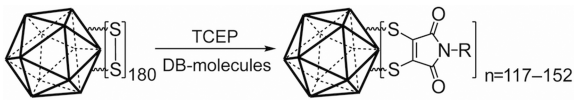

Name	R	Modification (%)	n
Qβ-Biotin	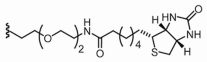	84.2 ± 0.18	152
Qβ-Azobenzene	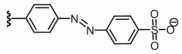	82.4 ± 4.0 *	148
Qβ-PEG	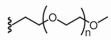	65.2 ± 0.94	117
Qβ-M		79.2 ± 1.4	143
Qβ-MA		75.3 ± 2.7	136
Qβ-N_3		78.2 ± 4.9	141
Qβ-Alkyne		75.8 ± 1.7	136

azide reaction may cause the reduction of azide to the amine via the Staudinger reaction. The reactivity of remaining azides on Qβ was further confirmed by click reaction with fluorescein−alkyne, which yielded 24 fluorescein moieties per capsid; see Figure S12.) We suspect the different yields are due to the nature of the functional groups, such as solubility in aqueous solution, and steric hindrance around the pore.[44,48,49] Importantly, electrophoretic analysis, discussed in detail below, show that the reaction principally reforms the higher-order oligomers (Figure 3A,B). In particular, we see the substantial reformation of the hexameric and pentameric

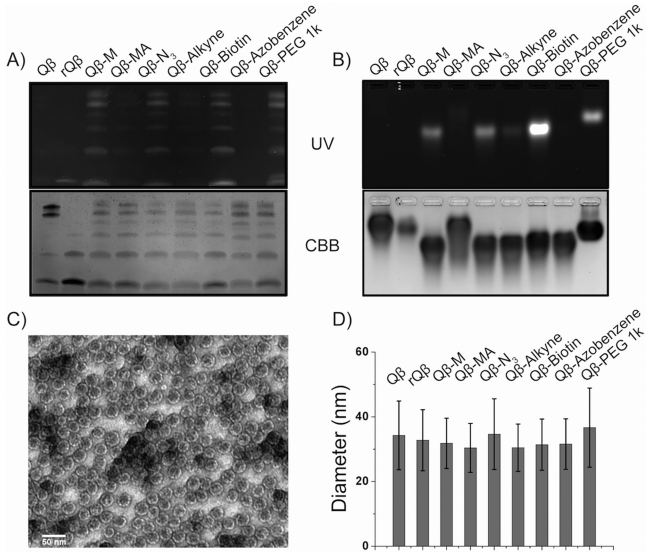

Figure 3. (A) Nonreducing SDS-PAGE of Qβ, reduced Qβ (rQβ), and Qβ−maleimide conjugates. (B) Native agarose gel of Qβ−maleimide conjugates. Both panels A and B are visualized by UV (top) and Coomassie brilliant blue (CBB) (bottom). (C) TEM micrograph of Qβ−alkyne conjugate. (D) DLS histogram of native Qβ, rQβ, and Qβ−maleimide conjugates in 0.1 M potassium phosphate buffer (pH 7.0).

subunits. This is significant, as intuitively, one would expect entropy to disfavor the reformation of these higher-order oligomers favoring instead a rebridging of both cysteines on a single protein to yield monomers. We tentatively suggest that this observation is attributed to a considerable amount of preorganization within the monomer, which facilitates a cross-linking back to the hexameric and pentameric subunits.

While dibromomaleimides have very little fluorescence, thiolated alkyl maleimides have been known to be fluorescent[51] and have recently been shown to be excellent small fluorophores in polymers.[52,53] This work inspired us to determine if the fluorescence was bright enough to serve a dual role as a functional handle as well as a small-molecule fluorophore. To that end, we conducted a photophysical evaluation of the reaction products and have plotted the excitation and emission spectra in Figure 4. Most of the conjugates were quite fluorescent in 0.1 M potassium phosphate buffer (pH 7.0), and all show an excitation, λ_{max}, near 400 nm and an emission, λ_{max}, between 538 and 548 nm. We could also clearly see the fluorescence when the conjugates were characterized by nonreducing SDS-PAGE (Figure 3A). We found this reaction to be very robust regardless of the functionalities and it produces stable conjugates, yet photophysical performance was highly dependent on the functional group.

Nonreducing SDS-PAGE reveals that hexamers and pentamers were reformed along with their lower-order subunits. As shown in Figure 3A, the bands are typically fluorescent under UV, and their position colocalizes with Coomassie brilliant blue (CBB) stain. The particle integrity was confirmed by native agarose gel electrophoresis (Figure 3B), morphology was confirmed by transmission electron microscopy (TEM), and dynamic light scattering (DLS) showed no change in particle diameter (Figure 3C,D). To confirm that the functionalization did not alter thermal stability, we conducted temperature-dependent circular dichroism (CD) experiments. Unfunction-

DOI: 10.1021/acs.bioconjchem.7b00305
Bioconjugate Chem. 2017, 28, 2277−2283

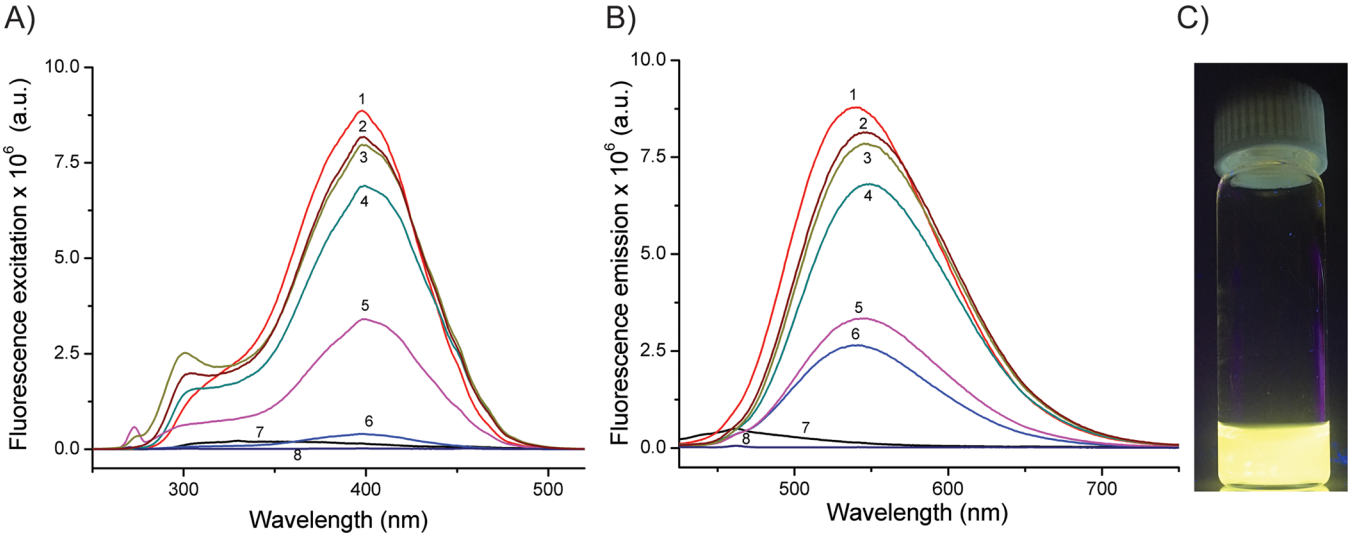

Figure 4. (A) Excitation and (B) emission spectra of Qβ−maleimide conjugates in 0.1 M potassium phosphate buffer (pH 7.0). The spectra are labeled thusly: (1) Qβ−M, (2) Qβ−PEG, (3) Qβ−biotin, (4) Qβ−N_3, (5) Qβ−alkyne, (6) Qβ−MA, (7) Qβ, and (8) Qβ−azobenzene. Excitation and emission maxima are around 400 and 540 nm, respectively. (C) Photograph of the reaction mixture of Qβ−PEG under 365 nm UV lamp illumination.

alized and mostly oxidized (~90%) Qβ has a temperature of denaturation (T_m) of 87.0 °C, and the fully reduced Qβ (rQβ) (T_m = 61.2 °C) shows attenuated thermal stability following disulfide bond reduction. As expected, after the disulfides were rebridged by DB compounds, the T_m returned to or exceeded the original VLP Qβ value (Figure S10).

When the reaction was visualized by a 365 nm UV light, it is clear that the reaction proceeds extremely quickly as the mixture immediately fluoresces yellow after reduced Qβ is added to the DB solutions (Figure 4C and Video S1). To quantify such quick kinetics, we turned to stopped-flow analysis, which revealed double exponential kinetics, which we ascribe to the two consecutive sulfur additions. The rates of the reaction were determined to have pseudo-first-order rate constants of 1.04 and 0.42 s^{-1} corresponding to half-lives of 670 and 1650 ms for each of the two bromine displacements by sulfur in the reaction, respectively (Figure S3 and Scheme S1).

Photophysical evaluation of the products yielded some interesting observations as well. Our initial efforts to quantify the yield of the reaction by fluorescence, using a water-soluble small molecule derived from Boc-protected cysteine and DB−PEG (Boc−Cys−PEG) as a standard, failed to give meaningful information. After investigation, we found the fluorescence intensity of the fluorophores, when attached to Qβ, are 48 times brighter than this small molecule standard we synthesized at the same relative concentration of fluorophore in the same media (Figure S6). Brightness is the product of quantum yield and extinction coefficient, and it is the parameter that we need to compare to explain the discrepancy. The quantum yield (Φ_F) of the standard Boc−Cys−PEG in water was found to be quite low at 1.36% and with an extinction coefficient of 260.6 L mol^{-1} cm^{-1}. On the other hand, on a per-chromophore basis, the extinction coefficient when attached to the capsid was found to be 2337.1 L mol^{-1} cm^{-1}, corresponding to a 9-fold increase. Indeed, it is quite likely that the Φ_F of the individual chromophores likewise increases. This is interesting and confirms similar reports of thiol−maleimide end groups on polymers, which were also 2−10 times brighter than the small molecular precursors.[53] While the excitation and emission wavelengths of the conjugates are inappropriate for in vitro work, they perfectly match with the commercially available filter set GFP-uv (λ_{ex}: 405 nm, λ_{em}: 500−540 nm) suggesting that they may serve as in vitro probes as well as a bespoke functional handle. Different from presynthesized fluorophores that are attached by bioconjugation reactions, the fluorescence of the probe we described here is generated as the bioconjugation reaction occurs. We qualitatively assessed the performance of two of the conjugates in cellular uptake studies with frequently used functional groups (Qβ−biotin and Qβ−PEG) and imaged the living cells by confocal laser microscopy. Chemically functionalized VLPs have shown differential uptake by macrophages,[54] which have implications in their use in targeting cells within the cancer microenvironment. Co-localization results in Figure 5 shows yellow fluorescence from the conjugates within mouse Raw-264.7 macrophages after incubating the particles for 4 h, successfully demonstrating that the maleimide conjugates can be tracked during cell uptake. An important caveat being that the fluorescent conjugates, once inside the cell, may transfer to cysteine rich substrates in late endosomes and lysosomes, likely concurrently with protolysis of the VLP. While this may or may limit their utility for certain applications, it could also be very useful for addressing the nature of the reducing environment and trafficking of digested substrates out of the late endosomes and lysosomes, an active area of research.[55−57] It may also be valuable in monitoring reduction-sensitive drug or biological macromolecule release within the reducing endosomal environment, an area of research we are presently pursuing with this technology.[58,59]

■ CONCLUSIONS

We have shown that we can functionalize the disulfides that line the pores of VLP Qβ with cationic, anionic, polymeric, and small-molecule functional handles. The conjugates are stable in serum following hydrolysis of the maleimide to the corresponding maleamic acid. The new conjugates were found to be equally, or more, stable than the oxidized capsid despite breaking and rebridging between 117−152 disulfides.

DOI: 10.1021/acs.bioconjchem.7b00305
Bioconjugate Chem. 2017, 28, 2277−2283

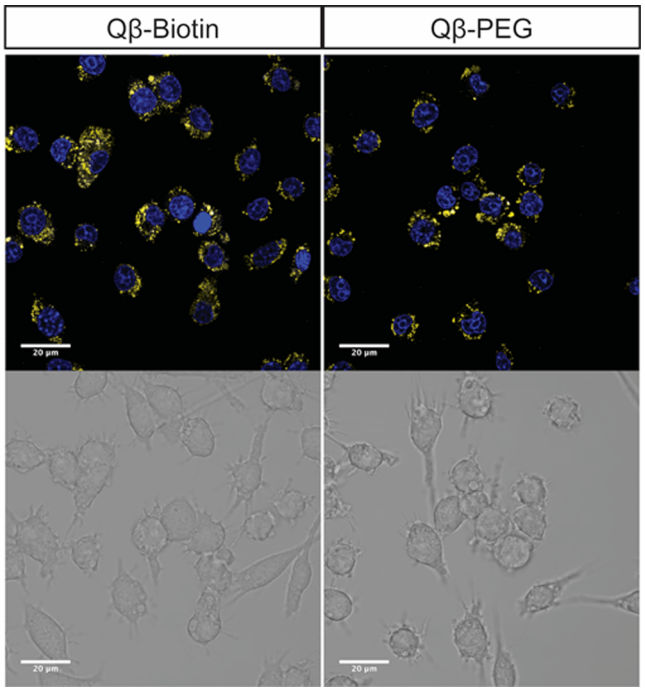

Figure 5. Confocal microscopy images of Qβ–maleimide conjugates in mouse Raw-264.7 cells: Qβ–biotin and Qβ–PEG. Top images: merged fluorescent channels. Bottom images: bright-field images. Color code: blue, NucRed Live 647 ReadyProbes Reagent; yellow, Qβ–maleimide particles.

The reaction is highly specific[45−47] and efficient, and the resulting label is highly fluorescent, which will aid in the visualization of their conjugates. As a result, these dibromomaleimide groups are a promising all-in-one functional handle and fluorescent label that can be applied in labeling applications in which chemical functionalization and cell tracking are of interest.

■ ASSOCIATED CONTENT

Supporting Information

The Supporting Information is available free of charge on the ACS Publications website at DOI: 10.1021/acs.bioconjchem.7b00305.

Detailed synthetic procedures and characterization of dibromomaleimide derivatives, Qβ expression and purification protocol, bioconjugation protocol, VLP conjugate thermal stability, reaction kinetics, photophysical study, confocal microscopy, transmission electron microscopy protocols, and serum stability studies. (PDF)

A video showing the Qβ dibromomalemide reaction. (AVI)

■ AUTHOR INFORMATION

Corresponding Author

*E-mail: gassensmith@utdallas.edu.

ORCID

Jeremiah J. Gassensmith: 0000-0001-6400-8106

Author Contributions

All authors have given approval to the final version of the manuscript. Z.C. and J.J.G. designed and conducted the experiments; Z.C., S.D.B., and D.D.W. conducted the protein purification and FPLC; Z.C., J.S.C., and G.M. conducted the kinetic studies; K.W.M. and S.D. conducted the high-resolution mass spectrometry; Z.C. and G.L.M. imaged cells; C.E.B. helped with the protein purification; and R.P.W. performed TEM imaging.

Funding

J.J.G. acknowledges the National Science foundation for their support (DMR-1654405), and G.M. acknowledges the Welch foundation for their support (AT-1935−20170325).

Notes

The authors declare no competing financial interest.

■ ACKNOWLEDGMENTS

We thank Dr. Xiuying Li and Prof. Zhenpeng Qin for providing the Raw 264.7 cell culture and discussion. We also thank Prof. Joseph Pancrazio, Prof. Theodore Price, and Dr. Bryan Black for confocal microscopy imaging.

■ REFERENCES

(1) Elsabahy, M., and Wooley, K. L. (2012) Nanoparticles for Biomedical Delivery Applications. *Chem. Soc. Rev. 41*, 2545−2561.

(2) Yoon, H. Y., Jeon, S., You, D. G., Park, J. H., Kwon, I. C., Koo, H., and Kim, K. (2017) Inorganic Nanoparticles for Image-Guided Therapy. *Bioconjugate Chem. 28*, 124−134.

(3) Zhang, N., Zhao, F., Zou, Q., Li, Y., Ma, G., and Yan, X. (2016) Multitriggered Tumor-Responsive Drug Delivery Vehicles Based on Protein and Polypeptide Coassembly for Enhanced Photodynamic Tumor Ablation. *Small 12*, 5936−5943.

(4) Abbas, M., Zou, Q., Li, S., and Yan, X. (2017) Self-Assembled Peptide- and Protein-Based Nanomaterials for Antitumor Photodynamic and Photothermal Therapy. *Adv. Mater. 29*, 1605021.

(5) Li, X., Che, Z., Mazhar, K., Price, T. J., and Qin, Z. (2017) Ultrafast Near-Infrared Light-Triggered Intracellular Uncaging to Probe Cell Signaling. *Adv. Funct. Mater. 27*, 1605778.

(6) Wen, A. M., and Steinmetz, N. F. (2016) Design of Virus-based Nanomaterials for Medicine, Biotechnology, and Energy. *Chem. Soc. Rev. 45*, 4074−4126.

(7) Chen, Z., Li, N., Li, S., Dharmarwardana, M., Schlimme, A., and Gassensmith, J. J. (2016) Viral Chemistry: The Chemical Functionalization of Viral Architectures to Create New Technology. *WIREs Nanomed. Nanobiotechnol. 8*, 512−534.

(8) Yildiz, I., Shukla, S., and Steinmetz, N. F. (2011) Applications of Viral Nanoparticles in Medicine. *Curr. Opin. Biotechnol. 22*, 901−908.

(9) Koudelka, K. J., Pitek, A. S., Manchester, M., and Steinmetz, N. F. (2015) Virus-Based Nanoparticles as Versatile Nanomachines. *Annu. Rev. Virol. 2*, 379−401.

(10) Lee, K. L., Shukla, S., Wu, M., Ayat, N. R., El Sanadi, C. E., Wen, A. M., Edelbrock, J. F., Pokorski, J. K., Commandeur, U., Dubyak, G. R., and Steinmetz, N. F. (2015) Stealth Filaments: Polymer Chain Length and Conformation Affect the *in vivo* Fate of PEGylated Potato Virus X. *Acta Biomater. 19*, 166−179.

(11) Longmire, M., Choyke, P. L., and Kobayashi, H. (2008) Clearance Properties of Nano-sized Particles and Molecules as Imaging Agents: Considerations and Caveats. *Nanomedicine 3*, 703−717.

(12) Prasuhn, D. E., Singh, P., Strable, E., Brown, S., Manchester, M., and Finn, M. G. (2008) Plasma Clearance of Bacteriophage Qβ Particles as a Function of Surface Charge. *J. Am. Chem. Soc. 130*, 1328−1334.

(13) Zeltins, A. (2013) Construction and Characterization of Virus-Like Particles: A Review. *Mol. Biotechnol. 53*, 92−107.

(14) Yin, Z., Comellas-Aragones, M., Chowdhury, S., Bentley, P., Kaczanowska, K., BenMohamed, L., Gildersleeve, J. C., Finn, M. G., and Huang, X. (2013) Boosting Immunity to Small Tumor-Associated Carbohydrates with Bacteriophage Qβ Capsids. *ACS Chem. Biol. 8*, 1253−1262.

DOI: 10.1021/acs.bioconjchem.7b00305
Bioconjugate Chem. 2017, 28, 2277−2283

(15) Pokorski, J. K., Breitenkamp, K., Liepold, L. O., Qazi, S., and Finn, M. G. (2011) Functional Virus-Based Polymer−Protein Nanoparticles by Atom Transfer Radical Polymerization. *J. Am. Chem. Soc. 133*, 9242−9245.
(16) ElSohly, A. M., Netirojjanakul, C., Aanei, I. L., Jager, A., Bendall, S. C., Farkas, M. E., Nolan, G. P., and Francis, M. B. (2015) Synthetically Modified Viral Capsids as Versatile Carriers for Use in Antibody-Based Cell Targeting. *Bioconjugate Chem. 26*, 1590−1596.
(17) Wang, Q., Chan, T. R., Hilgraf, R., Fokin, V. V., Sharpless, K. B., and Finn, M. G. (2003) Bioconjugation by Copper(I)-Catalyzed Azide-Alkyne [3 + 2] Cycloaddition. *J. Am. Chem. Soc. 125*, 3192−3193.
(18) Chen, Z., Li, N., Chen, L., Lee, J., and Gassensmith, J. J. (2016) Dual Functionalized Bacteriophage Qβ as a Photocaged Drug Carrier. *Small 12*, 4563−4571.
(19) Pokorski, J. K., Hovlid, M. L., and Finn, M. G. (2011) Cell Targeting with Hybrid Qβ Virus-Like Particles Displaying Epidermal Growth Factor. *ChemBioChem 12*, 2441−2447.
(20) Fiedler, J. D., Brown, S. D., Lau, J. L., and Finn, M. G. (2010) RNA-Directed Packaging of Enzymes within Virus-like Particles. *Angew. Chem., Int. Ed. 49*, 9648−9651.
(21) Molino, N. M., and Wang, S.-W. (2014) Caged protein nanoparticles for drug delivery. *Curr. Opin. Biotechnol. 28*, 75−82.
(22) Rohovie, M. J., Nagasawa, M., and Swartz, J. R. (2017) Virus-like particles: Next-generation nanoparticles for targeted therapeutic delivery. *Bioeng. Transl. Med. 2*, 43−57.
(23) Lohcharoenkal, W., Wang, L., Chen, Y. C., and Rojanasakul, Y. (2014) Protein Nanoparticles as Drug Delivery Carriers for Cancer Therapy. *BioMed Res. Int. 180549*.110.1155/2014/180549
(24) Rhee, J.-K., Hovlid, M., Fiedler, J. D., Brown, S. D., Manzenrieder, F., Kitagishi, H., Nycholat, C., Paulson, J. C., and Finn, M. G. (2011) Colorful Virus-like Particles: Fluorescent Protein Packaging by the Qβ Capsid. *Biomacromolecules 12*, 3977−3981.
(25) Hovlid, M. L., Steinmetz, N. F., Laufer, B., Lau, J. L., Kuzelka, J., Wang, Q., Hyypia, T., Nemerow, G. R., Kessler, H., Manchester, M., and Finn, M. G. (2012) Guiding plant virus particles to integrin-displaying cells. *Nanoscale 4*, 3698−3705.
(26) Zhao, X., Shen, Y., Adogla, E. A., Viswanath, A., Tan, R., Benicewicz, B. C., Greytak, A. B., Lin, Y., and Wang, Q. (2016) Surface Labeling of Enveloped Virus with Polymeric Imidazole Ligand-Capped Quantum Dots via the Metabolic Incorporation of Phospholipids into Host Cells. *J. Mater. Chem. B 4*, 2421−2427.
(27) Zhao, X., Cai, L., Adogla, E. A., Guan, H., Lin, Y., and Wang, Q. (2015) Labeling of Enveloped Virus via Metabolic Incorporation of Azido Sugars. *Bioconjugate Chem. 26*, 1868−1872.
(28) Chen, L., Wu, Y., Lin, Y., and Wang, Q. (2015) Virus-templated FRET Platform for the Rational Design of Ratiometric Fluorescent Nanosensors. *Chem. Commun. 51*, 10190−10193.
(29) Steinmetz, N. F., Hong, V., Spoerke, E. D., Lu, P., Breitenkamp, K., Finn, M. G., and Manchester, M. (2009) Buckyballs Meet Viral Nanoparticles: Candidates for Biomedicine. *J. Am. Chem. Soc. 131*, 17093−17095.
(30) Shukla, S., and Steinmetz, N. F. (2015) Virus-based nanomaterials as positron emission tomography and magnetic resonance contrast agents: from technology development to translational medicine. *WIREs Nanomed. Nanobiotechnol. 7*, 708−721.
(31) Datta, A., Hooker, J. M., Botta, M., Francis, M. B., Aime, S., and Raymond, K. N. (2008) High Relaxivity Gadolinium Hydroxypyridonate−Viral Capsid Conjugates: Nanosized MRI Contrast Agents. *J. Am. Chem. Soc. 130*, 2546−2552.
(32) Prasuhn, J. D. E., Yeh, R. M., Obenaus, A., Manchester, M., and Finn, M. G. (2007) Viral MRI contrast agents: Coordination of Gd by Native Virions and Attachment of Gd Complexes by Azide-Alkyne Cycloaddition. *Chem. Commun. 12*, 1269−1271.
(33) Garimella, P. D., Datta, A., Romanini, D. W., Raymond, K. N., and Francis, M. B. (2011) Multivalent, High-Relaxivity MRI Contrast Agents Using Rigid Cysteine-Reactive Gadolinium Complexes. *J. Am. Chem. Soc. 133*, 14704−14709.
(34) Hooker, J. M., O'Neil, J. P., Romanini, D. W., Taylor, S. E., and Francis, M. B. (2008) Genome-free Viral Capsids as Carriers for Positron Emission Tomography Radiolabels. *Mol. Imaging Biol. 10*, 182−191.
(35) Roldão, A., Mellado, M. C. M., Castilho, L. R., Carrondo, M. J. T., and Alves, P. M. (2010) Virus-Like Particles in Vaccine Development. *Expert Rev. Vaccines 9*, 1149−1176.
(36) Tissot, A. C., Renhofa, R., Schmitz, N., Cielens, I., Meijerink, E., Ose, V., Jennings, G. T., Saudan, P., Pumpens, P., and Bachmann, M. F. (2010) Versatile Virus-Like Particle Carrier for Epitope Based Vaccines. *PLoS One 5*, e9809.
(37) Hartmann-Boyce, J., Cahill, K., Hatsukami, D., and Cornuz, J. (2012) Nicotine Vaccines for Smoking Cessation. *Cochrane Database Syst. Rev. 8*.10.1002/14651858.CD007072.pub2
(38) Strable, E., Prasuhn, D. E., Udit, A. K., Brown, S., Link, A. J., Ngo, J. T., Lander, G., Quispe, J., Potter, C. S., Carragher, B., Tirrell, D. A., and Finn, M. G. (2008) Unnatural Amino Acid Incorporation into Virus-Like Particles. *Bioconjugate Chem. 19*, 866−875.
(39) Hovlid, M. L., Lau, J. L., Breitenkamp, K., Higginson, C. J., Laufer, B., Manchester, M., and Finn, M. G. (2014) Encapsidated Atom-Transfer Radical Polymerization in Qβ Virus-like Nanoparticles. *ACS Nano 8*, 8003−8014.
(40) Agarwal, P., and Bertozzi, C. R. (2015) Site-Specific Antibody−Drug Conjugates: The Nexus of Bioorthogonal Chemistry, Protein Engineering, and Drug Development. *Bioconjugate Chem. 26*, 176−192.
(41) Chalker, J. M., Bernardes, G. J. L., Lin, Y. A., and Davis, B. G. (2009) Chemical Modification of Proteins at Cysteine: Opportunities in Chemistry and Biology. *Chem. - Asian J. 4*, 630−640.
(42) Bundy, B. C., and Swartz, J. R. (2011) Efficient Disulfide Bond Formation in Virus-Like Particles. *J. Biotechnol. 154*, 230−239.
(43) Manzenrieder, F., Luxenhofer, R., Retzlaff, M., Jordan, R., and Finn, M. G. (2011) Stabilization of Virus-Like Particles with Poly(2-oxazoline)s. *Angew. Chem., Int. Ed. 50*, 2601−2605.
(44) Fiedler, J. D., Higginson, C., Hovlid, M. L., Kislukhin, A. A., Castillejos, A., Manzenrieder, F., Campbell, M. G., Voss, N. R., Potter, C. S., Carragher, B., and Finn, M. G. (2012) Engineered Mutations Change the Structure and Stability of a Virus-Like Particle. *Biomacromolecules 13*, 2339−2348.
(45) Jones, M. W., Strickland, R. A., Schumacher, F. F., Caddick, S., Baker, J. R., Gibson, M. I., and Haddleton, D. M. (2012) Polymeric Dibromomaleimides As Extremely Efficient Disulfide Bridging Bioconjugation and Pegylation Agents. *J. Am. Chem. Soc. 134*, 1847−1852.
(46) Smith, M. E. B., Schumacher, F. F., Ryan, C. P., Tedaldi, L. M., Papaioannou, D., Waksman, G., Caddick, S., and Baker, J. R. (2010) Protein Modification, Bioconjugation, and Disulfide Bridging Using Bromomaleimides. *J. Am. Chem. Soc. 132*, 1960−1965.
(47) Schumacher, F. F., Nobles, M., Ryan, C. P., Smith, M. E. B., Tinker, A., Caddick, S., and Baker, J. R. (2011) In Situ Maleimide Bridging of Disulfides and a New Approach to Protein PEGylation. *Bioconjugate Chem. 22*, 132−136.
(48) Lima, S. M. B., Vaz, A. C. Q., Souza, T. L. F., Peabody, D. S., Silva, J. L., and Oliveira, A. C. (2006) Dissecting the Role of Protein−Protein and Protein−Nucleic Acid Interactions in MS2 Bacteriophage Stability. *FEBS J. 273*, 1463−1475. Takamatsu, H., and Iso, K. (1982) Chemical Evidence for the Capsomeric Structure of Phage Qβ. *Nature 298*, 819−824.
(49) Golmohammadi, R., Fridborg, K., Bundule, M., Valegård, K., and Liljas, L. (1996) The Crystal Structure of Bacteriophage Qβ at 3.5 Å Resolution. *Structure 4*, 543−554.
(50) Nunes, J. P. M., Morais, M., Vassileva, V., Robinson, E., Rajkumar, V. S., Smith, M. E. B., Pedley, R. B., Caddick, S., Baker, J. R., and Chudasama, V. (2015) Functional Native Disulfide Bridging Enables Delivery of a Potent, Stable and Targeted Antibody-Drug Conjugate (ADC). *Chem. Commun. 51*, 10624−10627.
(51) Smith, T. L. Method for detecting molecules containing amine or thiol groups. U.S. Patent US4680272 A, July 14, 1987.

DOI: 10.1021/acs.bioconjchem.7b00305
Bioconjugate Chem. 2017, 28, 2277−2283

(52) Robin, M. P., and O'Reilly, R. K. (2014) Fluorescent and Chemico-Fluorescent Responsive Polymers From Dithiomaleimide and Dibromomaleimide Functional Monomers. *chem. sci. 5*, 2717−2723.
(53) Robin, M. P., Wilson, P., Mabire, A. B., Kiviaho, J. K., Raymond, J. E., Haddleton, D. M., and O'Reilly, R. K. (2013) Conjugation-Induced Fluorescent Labeling of Proteins and Polymers Using Dithiomaleimides. *J. Am. Chem. Soc. 135*, 2875−2878.
(54) Agrawal, A., and Manchester, M. (2012) Differential Uptake of Chemically Modified Cowpea Mosaic Virus Nanoparticles in Macrophage Subpopulations Present in Inflammatory and Tumor Microenvironments. *Biomacromolecules 13*, 3320−3326.
(55) Zhang, J., Yu, J., Jiang, J., Chen, X., Sun, Y., Yang, Z., Yang, T., Cai, C., Zhao, X., and Ding, P. (2017) Uptake Pathways of Guandinylated Disulfide Containing Polymers as Nonviral Gene Carrier Delivering DNA to Cells. *J. Cell. Biochem. 118*, 903−913.
(56) Schwarzländer, M., Dick, T. P., Meyer, A. J., and Morgan, B. (2016) Dissecting Redox Biology Using Fluorescent Protein Sensors. *Antioxid. Redox Signaling 24*, 680−712.
(57) van Kasteren, S. I., and Overkleeft, H. S. (2014) Endo-Lysosomal Proteases in Antigen Presentation. *Curr. Opin. Chem. Biol. 23*, 8−15.
(58) Meng, F., Hennink, W. E., and Zhong, Z. (2009) Reduction-Sensitive Polymers and Bioconjugates for Biomedical Applications. *Biomaterials 30*, 2180−2198.
(59) Xu, X.-D., Cheng, Y.-J., Wu, J., Cheng, H., Cheng, S.-X., Zhuo, R.-X., and Zhang, X.-Z. (2016) Smart and Hyper-Fast Responsive Polyprodrug Nanoplatform for Targeted Cancer Therapy. *Biomaterials 76*, 238−249.

DOI: 10.1021/acs.bioconjchem.7b00305
Bioconjugate Chem. 2017, 28, 2277−2283